



## Velocity analysis on CMP sections based on the smearing paradigm

D. L. Macedo, J. J. S. de Figueiredo, Rodrigo S. Portugal, State University of Campinas

Copyright 2009, SBGf - Sociedade Brasileira de Geofísica

This paper was prepared for presentation during the 11<sup>th</sup> International Congress of the Brazilian Geophysical Society, held in Salvador, Brazil, August 24-28 2009.

Contents of this paper were reviewed by the Technical Committee of the 11<sup>th</sup> International Congress of The Brazilian Geophysical Society and do not necessarily represent any position of the SBGf, its officers or members. Electronic reproduction or storage of any part of this paper for commercial purposes without the written consent of The Brazilian Geophysical Society is prohibited.

### Abstract

**Techniques that use Common Mid-Point (CMP) data, such as NMO correction, stacking and velocity analysis are the core of seismic processing. They are combination of procedures that relies on the physics, signal processing and basic laws of statistics. In general they all use a underlying velocity model, which gives a travelttime expression, and numerical schemes to accomplish their goals. For instance the construction of coherence panels in spectral velocity domain are traditionally made by summing up amplitudes along auxiliary hyperbolae, which are parameterized by zero-offset time and velocity. In this work we investigate how some of these methods could benefit of smearing procedures instead of stacking ones.**

### Introduction

CMP-based techniques, such as NMO correction, stacking and velocity analysis, are considered the core of seismic processing, mainly because their products will feed more advanced and critical procedures, such as migration and inversion. As a matter of fact, errors during the early stages of seismic processing often accumulate, generating mispositioned reflectors and bad geologic interpretation.

All these techniques have in common that, in general, they are all theoretically based on velocity model assumptions, associated to a travelttime expression, which is obtained from a combination of procedures that relies on the physics of waves and geometrical optics. The design of the actual technique from the theoretical model employs numerical schemes that are based on signal processing, basic laws of statistics and numerical analysis. For instance, the simplest form of velocity analysis is based on a layered geological model, in which the layers are homogeneous and separated by flat interfaces. The associated travelttime expression is the hyperbolic travelttime formula, which is dependent of the offset and is parameterized by RMS velocity and zero-offset travelttime, both obtained from the model. Also the numerical scheme is based on the semblance formula, which is, roughly speaking, a quotient between the squared sum of amplitudes and sum of squared amplitudes collected along hyperbolic curves.

Although velocity analysis using CMP sections is already a well established procedure, it has been studied thoroughly since its formal introduction by Taner and Koehler (1969). Historically, there is a number of modifications and extensions to the original idea, all of them improving or changing the geologic model and/or the coherence measurements.

Concerning improvements related to the geologic model or travelttime expression there is, for instance, the inclusion of anisotropy factors (Alkhalifah and Tsvankin, 1996), the geometrical correction of travelttime curves (de Bazelaire, 1988) or considering non hyperbolic curves (Abbad et al., 2009). On the other hand, concerning the improvements that address coherence measurements, we can cite, for example, the improvement of statistical measurements of coherence (Neidell and Taner, 1971) and the introduction of differential semblance (Li and Symes, 2007).

Great part of imaging process has its theoretical basis on integrals computed along auxiliary curves, such as Kirchhoff migration (Hubral et al., 1996; Tygel et al., 1996) or tau-p transforms (Clayton and McMechan, 1981). Actually these theoretical integrals are the reason why stacking amplitudes along auxiliary curves gives good results. Also, we can understand stacking amplitudes as the direct translation of theoretical formulas to practical problems, where the integral operation changes into discrete summation.

The usual methods of velocity analysis, as well as its variants and extensions, are all designed under the same principle, which we generically refer to *stacking* and which it can be divided in three parts:

**Location** Consider a travelttime function which is geometrically equivalent to a line (or surface);

**Measurement** Design some statistical measurement that gives some desired property, such as coherency;

**Stacking** On the intersection of *Location* and the data section, apply the *Measurement*.

Therefore, by the term “stacking”, we mean to perform numerical computation using the data collected along a curve defined by the travelttime expression. For instance the construction of coherence panels in spectral velocity (SV) domain are usually made by properly summing up squared amplitudes along auxiliary hyperbolae, which are parameterized by  $t_0$  and  $v$ .

In this work we propose a change of paradigm, which is to perform velocity analysis on coherence panel constructed by smearing instead of stacking. The smearing paradigm is not new, however, for it can be seen as a good alternative to stacking data on auxiliary curves, the way is performed in Kirchhoff migration. In this case, the smearing paradigm means that the amplitudes of seismic traces are smeared along isochrons in the migrated image (Santos et al., 2000). Actually, Kirchhoff migration by smearing can be seen as memory saving way to perform migration on massively pre-stack data, because each trace can be used only once, one independent of another, being a potential for parallel algorithms.

In the proposed method, we use the conventional geological model and travelttime expression, i.e., we consider a RMS

velocity model and the hyperbolic traveltimes expression. Also, as coherence measurement we choose the semblance as a starting formula. The main difference is that the CMP data is no longer summed along hyperbola to produce a semblance value on a single point of spectral velocity panel, but the amplitude of each sample of CMP section is spread along proper curves that lie on spectral velocity panel.

### Family of hyperbola

In order to build the smearing curve corresponding to a single point in CMP section, we have to consider a family of hyperbola which passes on this point. The well-known basic formula of hyperbolic traveltimes is

$$t^2 = t_0^2 + (x/v)^2, \quad (1)$$

where  $t$  is the reflection time,  $t_0$  is the zero-offset time,  $x$  is the offset and  $v$  is the medium velocity. The above formula tells us that for each  $(v, t_0)$  pair in SV domain there is a hyperbolae in CMP domain and vice-versa.

To develop our approach, we seek a family of hyperbola which intersection is at a given point  $(x_i, t_i)$ . In this way, we simply require that the parameters  $t_0$  and  $v$  must satisfy

$$t_i^2 = t_0^2 + (x_i/v)^2. \quad (2)$$

Isolating  $t_0$  we obtain a relationship

$$t_0^2 = t_i^2 - (x_i/v)^2, \quad (3)$$

where we require that  $v \geq x_i/t_i$ . Therefore inserting (3) in (1), we obtain a general equation

$$t^2 = t_i^2 - (x_i/v)^2 + (x/v)^2 \quad (4)$$

that represents a family of hyperbola that intersect at  $(x_i, t_i)$ , in which  $v$  is the family parameter. Figure 1(a) shows a family of hyperbola intersecting one point.

Each hyperbolae of the family of intersecting hyperbola can be represented as a point  $(v, t_0)$  at the SV domain. Therefore, the family of hyperbola described by (4) can be represented by a curve at the SV domain given by

$$t_0 = f(v) = \sqrt{t_i^2 - (x_i/v)^2}, \quad (5)$$

where  $v$  must be greater than  $x_i/t_i$ . Figure 1(b) shows the line that represents the family of hyperbola depicted in Figure 1(a). Notice that each colored hyperbolae depicted in Figure 1(a) has a one-to-one correspondence to a point, depicted as circle of the same color, depicted in Figure 1(b).

Therefore, for each point  $(x_i, t_i)$  in CMP domain, we can establish an one-to-one relationship to a curve  $\Gamma_i$  in SV domain, i.e.,

$$(x_i, t_i) \longleftrightarrow \Gamma_i,$$

where  $\Gamma_i$  is defined as

$$\Gamma_i = \left\{ (v, t_0) \mid t_0(v) = \sqrt{t_i^2 - (x_i/v)^2}, \quad v \geq x_i/t_i \right\}, \quad (6)$$

in SV domain.

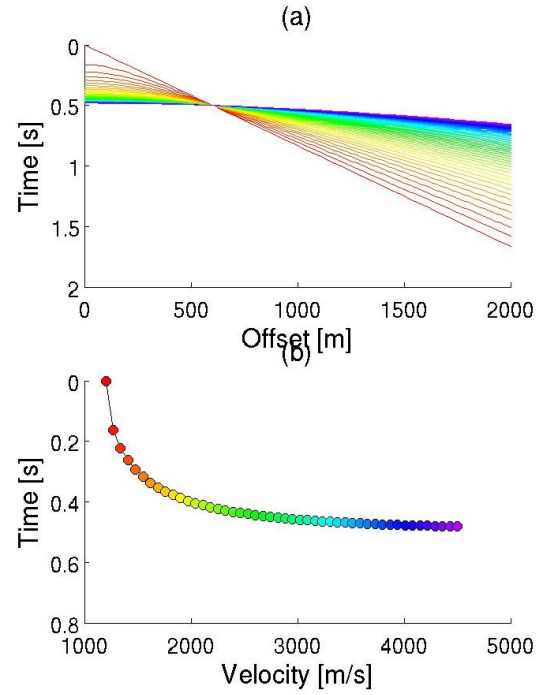


Figure 1: A family of hyperbola depicted on (a) intersect at one given point in CMP domain. Each hyperbolae of CMP domain depicted on (a) can be associated to point on SV domain (b), represented by a circle with the same color.

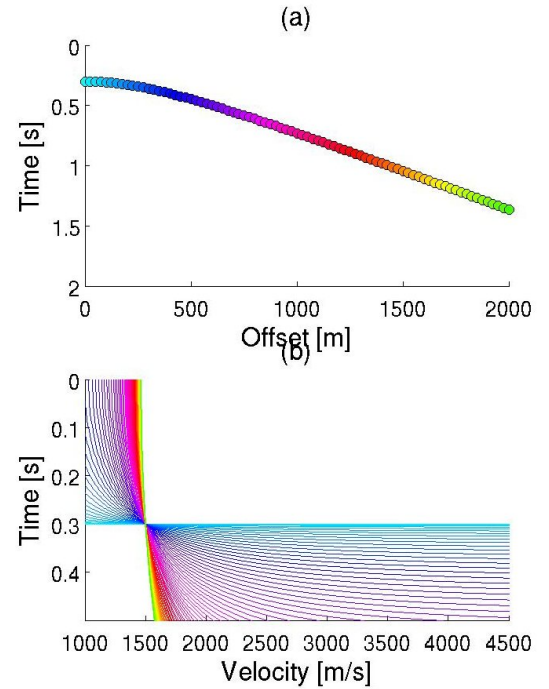


Figure 2: (a): Reflection event hyperbolae on CMP domain. (b): Smearing curves on SV domain. Each hyperbolae on the right is represented by a circle on CMP domain.

### Coherency panel by smearing

It is proposed the construction of a semblance-like coherence panel by smearing the amplitude and the squared amplitude

at the point  $(x_i, t_i)$  in CMP domain along the curve  $\Gamma_i$  in SV domain defined by (6).

As seen in Figure 2, each reflection event on CMP is related with a set of smearing curves that intersect on a point on SV domain which describes the event RMS velocity and ZO time.

In other to construct the coherence panel, the user must specify the velocity range for the SV domain; this is called trial velocity.

First of all, a panel is constructed by smearing the **amplitude** along the related smearing curves (*Smearred Amplitude Panel* – A panel). The amplitude is smeared in order to produce a constant amplitude density along the smearing curve length. The amplitude density is the relation between CMP point amplitude and the related curve length. The curve length is calculated from  $v \geq x_i/t_i$  to maximum trial velocity. At the process end, each point in the A panel must be squared.

At same time, another panel is constructed by smearing **squared amplitude** (*Smearred Squared Amplitude Panel* – S panel). In the same way before, a constant squared-amplitude density along the smearing curve is sought.

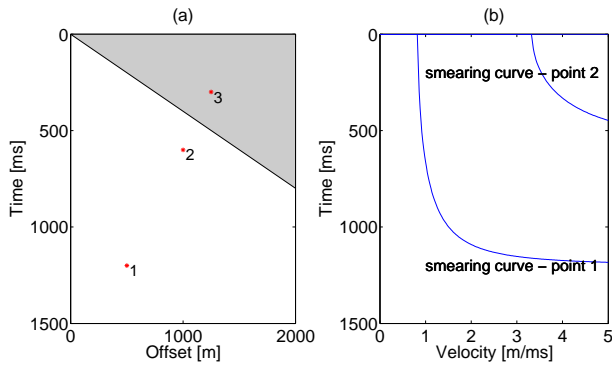


Figure 3: (a): Points in CMP domain; point 3 is in the area that produces no smearing curves. (b): Smearing curves on SV domain.

In both panels, the restriction in equation (6) –  $v \geq x_i/t_i$  – together with the maximum trial velocity, defines an area in CMP domain where the amplitude is not smeared. See Figure 3.

For deeper reflectors and higher RMS layer velocity a minimum offset is required in order to clearly define the intersection point in SV domain – called, from now on, *spots*. Figure 4 shows the reason. If the offset is not long enough, the coherence spot at the A panel produced by the summation of the amplitudes is not strong. At the same time, where there should not be a significant value at the panel due to non-coherent summation, there it is. To prevent this, the relation below must be satisfied:

$$x_{min} \sim v_h t_h, \quad (7)$$

where  $v_h$  and  $t_h$  are the higher expected RMS velocity and ZO time, respectively.

The *Semblance-like Coherence Panel* – C panel – is obtained by calculating the ratio between each point in the A panel and its corresponded at the S panel. Each ratio gives rise to a point in the C panel.

### Syntetic data example

In order to evaluate the proposed methodology, we present an example with synthetic data. They were generated analytically

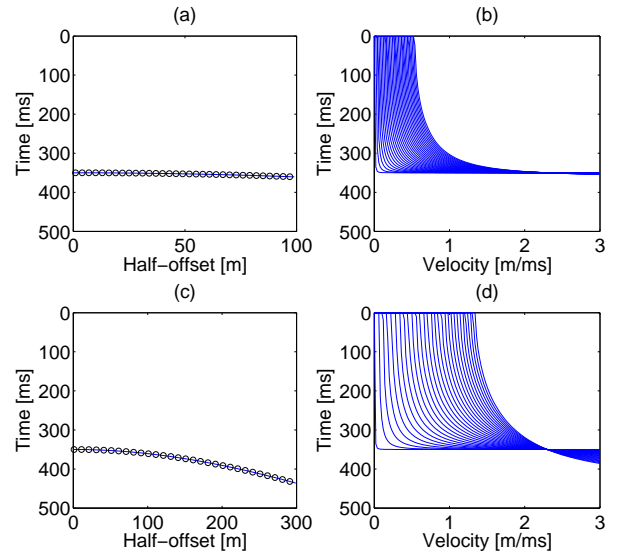


Figure 4: (a) and (b): reflection event hyperbolae on CMP domain and smearing curves on SV domain. (c) and (d): same event, with broader offset. Each hyperbolae on the right is represented by a circle on CMP domain.

by using the traveltime given by (1) with Ricker wavelet of 50 ms and unitary amplitude.

### Horizontally multi-layered media with noise

The used model was a horizontally multi-layered media with four flat reflectors. The layer velocities are, respectively, in downward direction,  $v_1 = 1$  m/ms,  $v_2 = 1.5$  m/ms,  $v_3 = 1.7$  m/ms e  $v_4 = 2.3$  m/ms (see Figure 5). Uniform random noise was added to seismic section (see Figure 6). The signal-to-noise ratio (*SNR*) is 0.104 dB<sup>1</sup>.

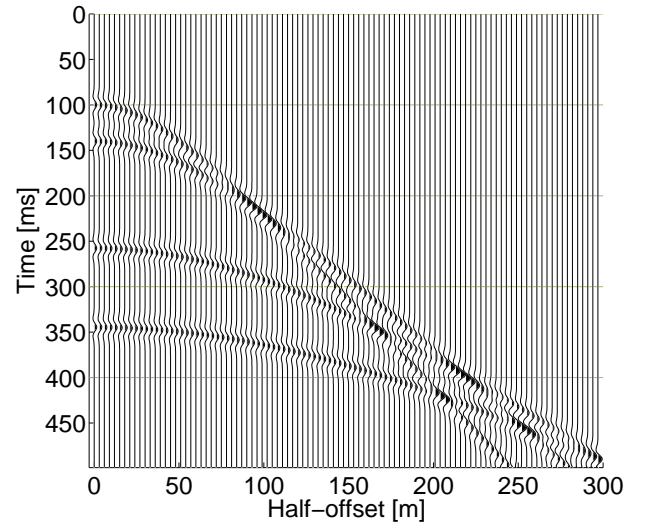


Figure 5: Multi-layered media CMP section with no noise. Clearly four hyperbolic events can be observed.

<sup>1</sup>  $SNR = 10 \log_{10} \left( \frac{\sum_k u^2(k)}{\sum_k n^2(k)} \right)$ , where  $u$  is the signal and  $n$  the noise.

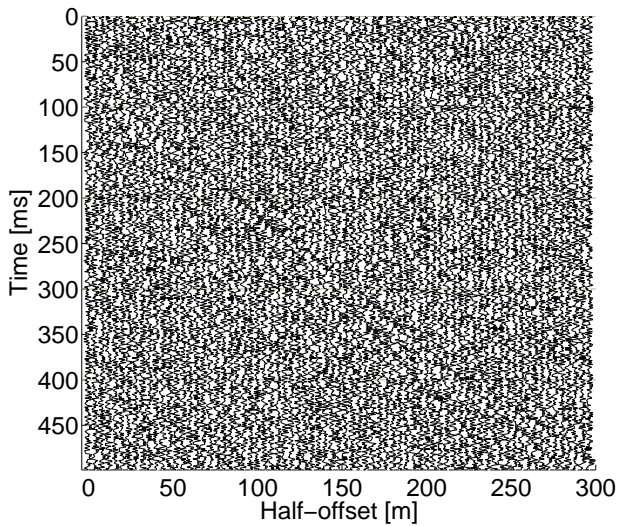


Figure 6: Multi-layered media CMP section, noise added.

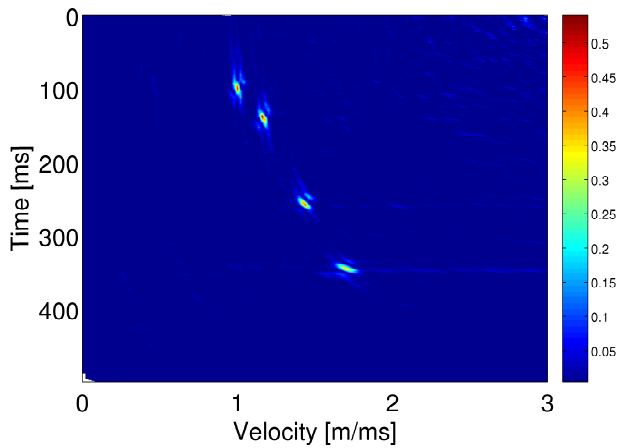


Figure 7: Coherence panel with spots showing the expected RMS velocities and ZO times.

Figure 7 shows the semblance-like coherence panel produced by the proposed method. In this panel the coordinated of local maxima give the expected RMS velocities and ZO times (see Table 1).

Table 1: Expected and obtained ZO times and RMS velocity

Layers	ZO time[s]		RMS velocity[m/ms]	
	expected	obtained	expected	obtained
1	100.0	100	1.000	1.000
1,2	140.0	138	1.165	1.160
1,2,3	257.7	259	1.434	1.440
1,2,3,4	344.6	345	1.695	1.700

## Summary and Conclusions

This work proposes a velocity analysis by means of a semblance-like coherence panel constructed by smearing amplitudes of a CMP section. This construction is made by accumulating amplitudes along curves on the spectral velocity domain that can be interpreted as the impulse response of a point on CMP section. The example shows that coherence

panel generated by the proposed method produces very accurate RMS velocities, indicating that it can replace the original summation method.

## References

- Abbad, B., B. Ursin, and D. Rappin, 2009, Automatic nonhyperbolic velocity analysis: *Geophysics*, **74**, U1–U12.
- Alkhalifah, T. and I. Tsvankin, 1995, Velocity analysis for transversely isotropic media: *Geophysics*, **60**, 1550–1566.
- Clayton, R. W. and G. A. McMechan, 1981, Inversion of refraction data by wave field continuation: *Geophysics*, **46**, 860–868.
- de Bazelaire, E., 1988, Normal moveout revisited: Inhomogeneous media and curved interfaces: *Geophysics*, **53**, 143–157.
- Hubral, P., J. Schleicher, and M. Tygel, 1996, A unified approach to 3-D seismic reflection imaging, Part I: Basic concepts: *Geophysics*, **61**, 742–758.
- Li, J. and W. W. Symes, 2007, Interval velocity estimation via nmo-based differential semblance: *Geophysics*, **72**, U75–U88.
- Neidell, N. S. and M. T. Taner, 1971, Semblance and other coherency measures for multichannel data: *Geophysics*, **36**, 498–509.
- Santos, L. T., J. Schleicher, M. Tygel, and P. Hubral, 2000, Modeling, migration, and demigration: *The Leading Edge*, **19**, 712–715.
- Taner, M. T. and F. Koehler, 1969, Velocity spectra: digital computer derivation and applications of velocity functions: *Geophysics*, **34**, 859–881.
- Tygel, M., J. Schleicher, and P. Hubral, 1996, A unified approach to 3-D seismic reflection imaging, Part II: Theory: *Geophysics*, **61**, 759–775.

## Acknowledgments

The authors would like to thank CAPES and CNPq for financial support. R. S. Portugal also thanks the Research Foundation of the State of São Paulo (FAPESP) for the financial support provided by grant 05/03769-7.